Evidence of Lipid Exchange in Styrene Maleic Acid Lipid Particle (SMALP) Nanodisc Systems

Journal:	*Langmuir*
Manuscript ID	la-2016-02927s.R1
Manuscript Type:	Article
Date Submitted by the Author:	n/a
Complete List of Authors:	Hazell, Gavin; University of Bristol, Chemistry Arnold, Thomas; Diamond Light Source, Tognoloni, Cecilia; University of Bath, Chemistry Department Barker, Robert; University of Dundee, School of Science and Engineering Clifton, Luke; Rutherford Appleton Laboratory, ISIS Steinke, Nina-Juliane; Rutherford Appleton Laboratory, ISIS Edler, Karen; University of Bath, Chemistry Department

Evidence of Lipid Exchange in Styrene Maleic Acid Lipid Particle (SMALP) Nanodisc Systems

Gavin Hazell [a†], *Thomas Arnold* [b], *Robert D. Barker* [c], *Luke A. Clifton*[d], *Nina-Juliane Steinke*[d], *Cecilia Tognoloni* [a], *and Karen J. Edler* [a]

[a] Department of Chemistry, University of Bath, Claverton Down, Bath, BA2 7AY, UK

[b] Diamond Light Source, Harwell Science and Innovation Campus, Didcot, OX11 ODE, UK

[c] School of Science and Engineering, University of Dundee, Dundee, DD1 4HN, UK

[d] ISIS Spallation Neutron Source, STFC, Harwell Science and Innovation Campus, Didcot, OX11 OQX, UK.

Abstract

Styrene-alt-Maleic Acid lipid particles (SMALPs) are self-assembled discoidal structures composed of a polymer belt and a segment of lipid bilayer, which are capable of encapsulating membrane proteins directly from the cell membrane. Here we present evidence of the exchange of lipids between such "nanodiscs" and lipid monolayers adsorbed at either solid-liquid or air-liquid interfaces. This behavior has important implications for the potential uses of nanodiscs.

Introduction

The term nanodisc has recently been coined to describe self-assembled soluble disc-like structures of phospholipid stabilized by a protein or polymer 'belt'[1, 2, 3]. They have been developed as a method of solubilizing membrane proteins incorporated into the bilayer. Membrane proteins make up a considerable percentage of the proteome (around 30 %) and account for 70 % of therapeutic targets[4]. However these proteins, which are inherently insoluble in water, are challenging to crystallize[5]. Solubilizing these proteins using nanodiscs offers the possibility for studying membrane proteins in solution using well-established techniques such as Dynamic Light Scattering (DLS) or Small Angle X-ray & Neutron Scattering (SAXS/SANS). It has also been argued that membrane proteins encapsulated in nanodiscs may be crystallized and thereby allow crystallographic studies[6, 7, 8].

The first nanodisc structure to be made was based on amphipathic helical proteins[9, 10] which were termed 'membrane scaffold proteins' (MSP's). The MSP's wrap around the phosphiolipid tails like a belt to form well defined disc-like shapes that are highly monodisperse. These systems have now been extensively studied in solution by small-angle-scattering including systems with[11, 12] and without[13, 14] encapsulated membrane proteins.

Another potential method for studying membrane proteins within nanodiscs is to use surface scattering techniques[15, 16]. This approach requires the adsorption of the protein containing nanodiscs at an interface, which can be probed with x-rays and/or neutrons to give information regarding structural changes that depend on conditions. Recently the interaction of MSP nanodiscs with both air-liquid[8] and solid-liquid[6] interfaces has been studied using neutron reflectometry. MSP nanodiscs were shown to adsorb upon positively charged lipid monolayers at the air-water interface with their bilayer parallel to the lipid monolayer. Similarly adsorption at

the silica-water interface has shown MSP nanodisc layers oriented parallel to the interface. The same group have also shown that it is possible to adsorb layers of nanodiscs containing an encapsulated membrane protein (cytochrome P450 reductase)[7, 17]. Here it was shown that the membrane protein maintained its biological function even when adsorbed at the solid-liquid interface.

More recently another method for making nanodiscs was developed, based upon a styrene-alt-maleic acid (SMA) polymer belt[18, 19]. Although not as monodisperse as the MSP discs, these polymer discs (also known as "SMA lipid particles" or SMALPs) have a well-defined size and discoidal shape which are capable of spontaneously self-assembling in the presence of dispersed phospholipid and pH > 8. The major advantage of such polymer-stabilized systems over the protein-stabilized analogues is their ease of preparation. The polymer can be directly combined with the cell line in which the membrane protein of interest has been over-expressed. The polymer then self-assembles with phospholipids and the membrane protein directly from the cell membrane. This allows the process to be conducted in one step and negates the need for detergent extraction and subsequent purification associated with the protein-stabilized systems[19, 20, 21, 22].

Despite a number of studies showing the interfacial adsorption of nanodiscs stabilized by a protein belt, no such studies exist for the polymer-stabilized systems. It was with this in mind that we began a study of whether polymer-stabilized nanodiscs could be adsorbed at interfaces in a manner similar to that already observed for protein based discs. However, these systems have some complications that have made our initial experiments more interesting than anticipated. In particular we have found evidence of fast (on the timescale of our experiments) lipid exchange between the nanodiscs and lipid monolayers, something that is of particular relevance for some

of the potential uses of nanodiscs containing membrane proteins going forward. The functionality of many membrane proteins is related to the local lipid environment in the membrane[23, 24]. The use of SMALPs to extract proteins directly from native membranes should, in principal, also extract any associated lipids and thereby retain functionality in solution. The ability to subsequently control the lipid environment via lipid exchange, then, may give us an opportunity to directly test how dependent a protein is on this local lipid environment. This final objective is clearly a complex one, so the first steps to understanding lipid exchange in these systems is to study the behavior in nanodiscs without proteins.

In this article we present neutron scattering measurements that show the exchange of protonated with deuterated lipids between nanodiscs in solution and lipid monolayers at both the air-water and silicon-water interface. We have examined systems with a range of different lipids including both zwitterionic and cationic lipid monolayers, and nanodiscs that include both neutral phosphatidylcholine (PC) and negatively charged phosphorylglycerol (PG) lipids.

Experimental Section

Materials

HCl, NaOH, styrene, maleic anhydride, 2-(dodecylthiocarbonothioylthio)-2-methylpropanoic acid (DDMAT), *α,α′*-azoisobutyronitrile (AIBN), dioxane, 2-oleoyl-1-palmitoyl-*sn*-glycero-3-phosphocholine (POPC) and dioctadecyldimethylammonium bromide (DODAB) were all purchased from Sigma-Aldrich (U.K). All were purchased at a purity level of 96 % or higher and generally used without further purification. The only exceptions were AIBN which was re-crystallised from methanol and styrene which was purified using a silica column to remove the inhibitor. 1,2-dioleoyl-*sn*-glycero-3-phosphocholine (DOPC), 1,2-dimyristoyl-d54-*sn*-glycero-3-phosphocholine (d-DMPC) and 1,2-dimyristoyl-d54-*sn*-glycero-3-[phospho-*rac*-(1-glycerol)]

(sodium salt) (d-DMPG) were purchased from Avanti Polar Lipids (U.S.A). They were purchased at purity levels of 99 % (and 98 % atom D) and were also used without further purification.

Methods

Polystyrene-alt-maleic acid (SMA) co-polymer Synthesis

The SMA co-polymer was prepared according to Harrison et al[25]. 500 mg of styrene, 202 mg of maleic anhydride, 3.8 mg of DDMAT, 3.43 mg of AIBN and 0.7 ml of dioxane were added to a sealed single necked round bottom flask with a magnetic stirrer under an N_2 atmosphere. The content within the flask was de-gassed and re-filled with N_2 via three consecutive freeze-thaw cycles. The flask was covered with aluminium foil to avoid radical initiator (AIBN) degradation. The solution was then heated to 60 °C with stirring for 21 hours and then allowed to cool to room temperature. Once cooled the polymer was precipitated in ice-cold diethyl ether three times. The precipitate was collected using a Buchner filter and a nylon filter. This was then freeze-dried under vacuum overnight at a temperature of -40 °C. This resulted in the synthesis of polystyrene-co-maleic-anhydride. The precipitate was then converted to polystyrene-co-maleic acid via reflux under basic conditions. The polystyrene-co-maleic-anhydride was added to 50 ml of a 2 M NaOH solution and refluxed for 3 hours. The solution was allowed to cool to room temperature. Added dropwise to this was 500 ml of a 2 M HCl solution. The resultant cloudy mixture was then centrifuged at 5000 rpm for 10 minutes where a polymer pellet formed at the bottom of the centrifuge tube. The pellet was then re-dissolved in a small amount of 2 M HCl and centrifuged once more. This process was repeated three times in total. The final polymer pellet was then dissolved in a minimum amount of 1 M NaOH and freeze dried overnight. NMR and GPC were used to confirm polymer synthesis, with an average molecular weight of 6.7 kDa

and PDI of 1.14, examples of which can be found in the supporting information accompanied with this article.

Nanodisc Preparation

Nanodiscs were prepared according to Jamshad et al[18, 22]. A 0.5 wt % lipid solution was made by adding 0.025 g of the relevant phospholipid(s) to 3.92 ml of buffer (50 mM phosphate buffer, 200 mM NaCl, pH 8). This solution was sonicated for 10 minutes to enable lipid dispersion within the buffer. 1.08 ml of a 6.5 wt % polystyrene-co-maleic acid solution in buffer was then added to the lipid suspension, giving a final polymer concentration of 1.5 wt %. This solution was agitated by hand for 5 minutes in order to accelerate the self-assembly process. At the end the solution was completely clear, which has been shown to indicate the formation of nanodiscs[18]. The presence of discs was confirmed by DLS (see supporting information). No other species were observed in solution in the DLS measurements so further purification was not needed.

Langmuir Trough Studies

Monolayers of the lipids POPC or DODAB were prepared by the deposition of a 100 μl solution (0.5 mg ml^{-1} in chloroform) over a phosphate buffer sub-phase (50 mM phosphate buffer, 200 mM NaCl). Ten minutes was allowed for chloroform evaporation. Surface pressure-time measurements were carried out using a Nima Technology type 611 Langmuir trough, using a 1 cm wide Wilhelmy plate sensor. The monolayer was compressed and held to a surface pressure of 15 mNm^{-1} using a double barrier compression system at a rate of 20 cm^2 min^{-1}. The monolayer was allowed to equilibrate for 5 minutes, at which point the nanodisc solution was injected beneath the barrier. Surface pressure evolution with time was monitored until the surface pressure began to plateau.

Neutron Reflectometry

The details of the theory of Neutron Reflectometry (NR) are well established and we refer the reader to the literature for a more detailed description of these techniques[26, 27]. Here we restrict our description to a brief outline of the key features that are important for the interpretation of our results. The specular reflection of neutrons is measured as a function of the scattering vector, Q, which lies perpendicular to the surface normal ($Q = (4\pi/\lambda) \sin\theta$), where θ is the angle of reflection and λ is the wavelength of the neutron beam). The experimental reflectivity is therefore related to the scattering length density of the material ($\rho = \sum_i n_i b_i$, where n is the number of nuclei, i, in a given volume and b is the coherent scattering length of that nuclei) through an inverse Fourier transform[28]. The technique relies on the fact that neutrons interact with the nuclei of the sample under investigation, and in particular that the scattering lengths of hydrogen and deuterium are very different (-3.74 x 10^{-5} Å and 6.67 x 10^{-5} Å for hydrogen and deuterium respectively). By controlling the deuterium content it is possible to vary the contrast of different layers within a sample and thereby constrain subsequent fits to the experimentally observed scattering. This also allows particular sensitivity to the incorporation of deuterated material into an adsorbed monolayer at an interface composed of protonated material, a feature that we take particular advantage of in this work.

The interpretation of such scattering data is model-dependent. The phase rule means that it is not possible to directly extract the structure from the observed scattering pattern. Instead the scattering is compared with that calculated from a proposed model that is based on existing knowledge of the system under investigation. Therefore, in order to interpret the scattering data, it is crucial that we have some knowledge of the neutron scattering length density (SLD) of the

materials in the system. Based on these values and by limiting the models to physically realistic constraints, one can determine an SLD profile that can explain the scattering.

Many SLD values are available in the literature, based on years of experiments, but it is also possible to calculate the SLD for a given compound based on its molecular volume. The SLD values used in this work are shown in table 1. One can also calculate an SLD for a nanodisc based on the SLD's of its components. This is calculated as a function of the mole fraction of lipid(s) and polymer[29]:

$$\rho_{nanodisc} = (\rho_{SMA} \cdot \chi_{SMA}) + (\rho_{LIPID} \cdot \chi_{LIPID})$$

where ρ_{SMA} and ρ_{LIPID} are the scattering length densities of the polymer and lipid respectively, whilst χ_{SMA} and χ_{LIPID} are their mole fractions. Our calculated values for the fully deuterated nanodiscs used in this study are also shown in Table 1

Table 1- Summary of calculated scattering length densities (from molecular volumes) used to model neutron reflectometry data.

Layer	Molecular Volume (Å^3)	SLD (x 10^{-6} Å^{-2})
PC Head group	268[30]	1.86
POPC Tails	934[31]	-0.21
DOPC Tails	985[32]	-0.21
DODAB	1174[33]	-0.32
d-DMPC	1101[34]	5.9
d-DMPG	1025[35]	5.9

OTS	542[36]	-0.35
SMA-polymer	-	1.89[18]
d-DMPC nanodisc	-	4.02

Table footnote: The POPC monolayer has been modelled using two layers which account for the lipid tail and head group separately [37]. DODAB is known to have a significantly smaller head group [33, 38] and so this was modelled using only one layer.

The air-liquid neutron reflectometry[16] experiments were conducted on the INTER beamline[39] and the solid-liquid experiments on the OFFSPEC beamline[40], both at the ISIS spallation source (Oxford, U.K). For both beamlines, the measurements used several fixed incidence angles (0.8° and 2.3° for INTER and 0.5, 1.0 and 2.0° for OFFSPEC). In both cases the absolute reflectivity was calibrated with respect to the direct beam and the reflectivity from a clean D_2O interface.

The neutron reflectometry data presented here is compared to reflectometry curves calculated from a model SLD profile using MOTOFIT[41, 42]. This software uses the Abeles optical matrix method[43] to calculate the theoretical reflectivity from a series of thin layers and allows the user to co-refine reflectometry data from multiple contrasts. In each case the model consists of several layers each generated from the following parameters; layer thickness (d), interfacial roughness (σ), SLD and solvent volume fraction (Φ). These parameters generate a profile showing the variation of SLD across the interface. The error associated with each model parameter can be estimated by varying each parameter separately and accepting the maximum deviation for which the calculated reflectivity still fits the experimentally observed data for all the corresponding isotopic contrasts[32].

For the air-water measurement, we have examined the interaction of a fully protonated monolayer of lipid (either zwitterionic POPC or cationic DODAB) spread from chloroform to a surface pressure of 15 mNm^{-1} on to the surface of a control buffer solution or a buffer solution containing nanodiscs made from fully deuterated lipids (100% d-DMPC or 25 % d-DMPG:d-DMPC, the latter introducing negative charge into the nanodisc). All measurements were conducted on a buffer, 50 mM phosphate and 200 mM NaCl, pH 8, and to achieve contrast variation, the measurements were repeated using either D_2O or ACMW (Air-contrast-matched-water; a mixture of H_2O and D_2O in the proportion that results in a net SLD of zero). The samples were contained in Teflon troughs (152 x 42 x 3 mm) and the surface pressure recorded prior to measurement (Nima technology surface pressure sensor). Neutron reflectometry measurements were then taken after an equilibration time of 40-60 minutes.

The silicon-water measurement used a standard sample cell[44] containing a silicon block (80 x 50 x 15 mm) that had been cleaned and coated with OTS using standard protocols[45, 46]. This yields a dense hydrophobic interface onto which a lipid monolayer can adsorb. After characterizing the OTS layer, a fully protonated lipid monolayer of zwitterionic DOPC was formed at the surface by vesicle fusion. This process is also a standard method for forming a lipid monolayer on hydrophobic surfaces[47, 48]. Again, after characterizing the monolayer in multiple buffer contrasts, 5 ml of solution containing nanodiscs made from fully deuterated lipids (100% d-DMPC prepared as above in H_2O) was injected. Approximately 30 minutes was then allowed for equilibration after which the nanodisc solution was rinsed with H_2O buffer. After measuring in this contrast the buffer was exchanged for D_2O and another measurement made. The total measurement time was 3.5 hours for all the contrasts after nanodisc injection.

Results and Discussion

Langmuir trough measurements

Figure 1 shows a plot of the surface pressure of a POPC and a DODAB monolayer on a solution containing (DMPC) nanodiscs. The lipids were initially spread from chloroform onto a clean buffer solution to a surface pressure of 15 mN m^{-1}. After a short settling time while the chloroform evaporated, the surface area was kept constant and the surface pressure monitored as a solution of nanodiscs was injected underneath the lipid film. After injection the concentration of nanodiscs in the sub-phase was of the order 10^{19} nanodiscs dm^{-3}. Since there are, on average, 202 lipids per nanodisc[49] we can safely assume that the number of lipids in solution far exceed the number on the surface (at 15mN m^{-1} the area per molecule of a PC lipid is approximately 50 $Å^2$, so for a trough surface area of approx. 200cm^2 we have around 10^{16} lipid molecules at the surface). As a control, the same experiment was repeated without injection of nanodiscs, and this data is also shown in Figure 1.

For both monolayer types, after injection of the nanodiscs we observed an initial drop followed by a substantial increase in the surface pressure. The initial drop in surface pressure is due to the perturbation of the monolayer associated with nanodisc injection. However, the subsequent increase is clear indication of a significant interaction of the nanodiscs with the monolayer. We note that the timescale (1-2 hours) for the surface pressure change is similar for both monolayer types but the DODAB system shows a larger total increase in pressure (up to 35 mNm^{-1}) than the POPC system (up to 25 mNm^{-1}). As we will discuss below, we believe that the rise in surface pressure is due to lipid transfer from the nanodiscs into the supporting lipid monolayer.

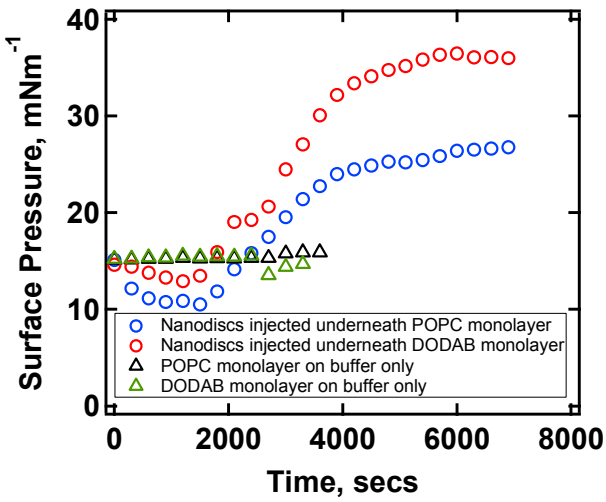

Figure 1- The variation of surface pressure with time for monolayers with an initial surface pressure of 15 mNm^{-1} and constant area. POPC monolayer on an aqueous buffer sub-phase (black), a sub-phase containing polymer-stabilized nanodiscs (blue) and a DODAB monolayer also on a sub-phase containing polymer-stabilized nanodiscs (red). Nanodiscs were injected at t = 0 seconds with the injection taking approximately 10 seconds.

Neutron Reflection

Figure 2 shows the neutron reflectometry and SLD profiles for h-POPC monolayers (15 mN m^{-1}) spread on the surface of a buffer solutions that do and do not contain deuterated nanodiscs (both 100% d-DMPC and 25% d-DMPG:d-DMPC). The parameters used to generate these SLD profiles shown in Table 2.

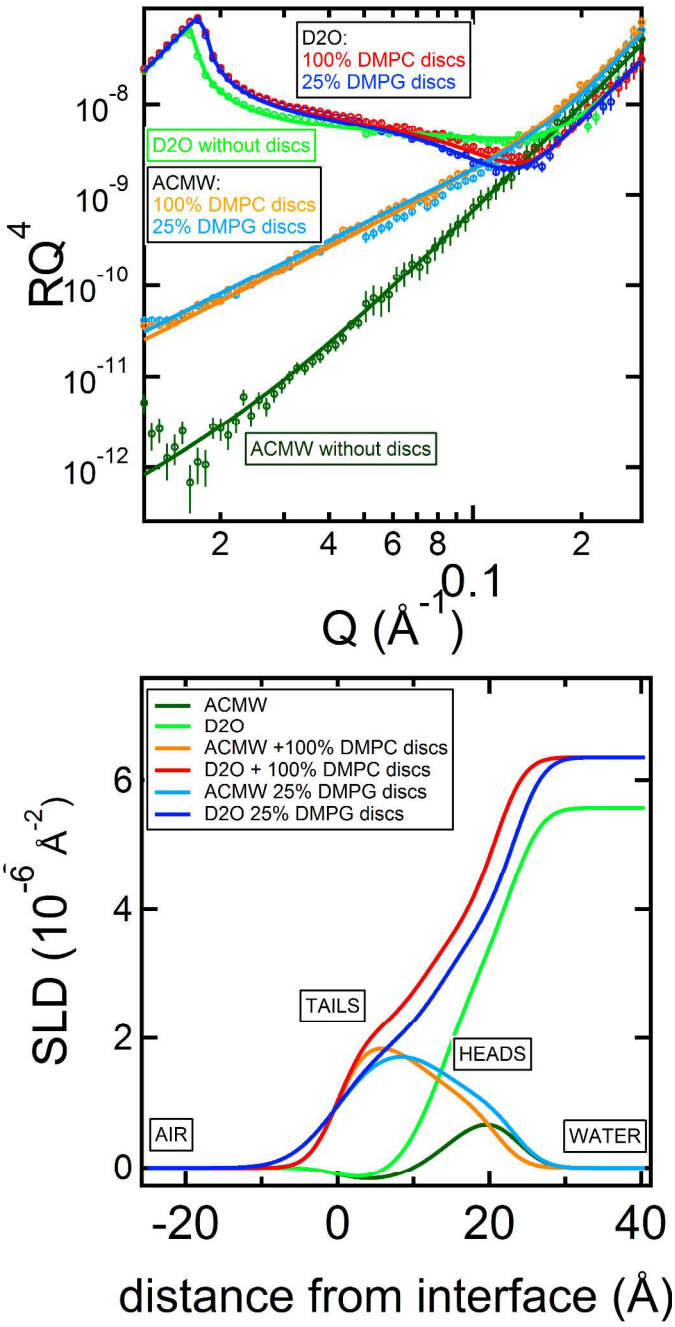

Figure 2- An h-POPC monolayer on ACMW (dark green) and D_2O (green) buffer contrasts without discs, and on buffer solutions containing 100% d-DMPC nanodiscs (ACMW: light blue and D_2O: dark blue) or 25 % DMPG:DMPC nanodiscs (ACMW: orange and D_2O: red))

Table 2 Structural parameters obtained from the best fit for h-POPC monolayers on the surface of buffer solutions with and without nanodiscs (for both D_2O and ACMW contrasts).

Sample	Layer	SLD ($\times 10^{-6}$ Å^{-2})	Thickness (Å)	Hydration (%)	Roughness (Å)
Buffer solution without discs	POPC tail	-0.21	14.5 ± 2	0	3 ± 2
	POPC head	1.86	9 ± 2	50± 7	5 ± 2
	D_2O Sub-phase	5.57	n/a	n/a	3 ± 2
	ACMW Sub-phase	0			
Buffer containing 100% d-DMPC disc	POPC tail	2.0 ± 0.5	12 ± 2	0	3 ± 2
	POPC head	1.86	9 ± 2	50±7	5 ± 2
	D_2O Sub-phase	6.35	n/a	n/a	3 ± 1
	ACMW Sub-phase	0			
Buffer containing 25% d-DMPG:d-DMPC discs	POPC tail	1.9 ± 0.4	14.5± 3	0	3 ± 2
	POPC head	1.86	9 ± 2	50± 8	5 ± 2
	D_2O Sub-phase	6.35	n/a	n/a	3 ± 1
	ACMW Sub-	0			

	phase				

On the buffer solution without discs, the POPC monolayer fits a simple two layer model that is consistent with the literature. Although we are unaware of any equivalent data for POPC monolayers on water, Wacklin et al have published data for a solid supported bilayer of POPC[50]. This suggests that the head region of a monolayer would be expected to be approximately 6Å and the tail approximately 12-13Å (i.e. around half a bilayer). Importantly our data for these contrasts is not very sensitive to the presence of the fully protonated POPC monolayer since the scattering is mostly governed by the solvated lipid head group. As such we cannot be confident in the accuracy of the details of this fit other than to say that it is consistent with previous results. However this approach does give us particular sensitivity to the potential interaction with nanodiscs containing deuterated lipids.

For both cases on buffer solutions containing nanodiscs a very significant difference is seen to the observed reflectivity on solutions without nanodiscs. This is particularly evident for the data on ACMW which each show a significant increase in scattering at low Q. Such behavior is only possible with a significant increase in the scattering length of the interface. There are several possible reasons for this that we will discuss below, but it is clear that the presence of nanodiscs of either type in the sub-phase has a big effect on the structure of the air-water interface.

We have considered a number of possible scenarios for the change in scattering. The two that we consider most likely are; a simple adsorption of intact nanodiscs beneath the POPC monolayer and the exchange of lipids between the monolayer and the nanodiscs (either adsorbed or in solution). Given the minimal number of contrasts available, we have applied the general principle of using the simplest model (fewest number of layers) to explain the data.

For the first of these scenarios, we have attempted to model the adsorption of nanodiscs by assuming that the POPC monolayer is unchanged and including an additional layer below this to account for the deuterated nanodiscs. The SLD of the nanodiscs was calculated as described earlier (see Table 1) and they have a well-defined size, determined from small angle scattering data[18, 49]. This size imposes a minimum thickness on the third layer of our model of ~30 Å, (effectively equivalent to a DMPC bilayer) and with this constraint we were unable to find an acceptable fit to the observed data. Instead the data can be reasonably modelled with a much thinner layer of the order 10Å that is not consistent with intact nanodiscs. An equally acceptable reflectivity profile can be simulated more simply by modifying the SLD's in the two-layer model of the "POPC" monolayer. Principally this requires a significant increase in the SLD of the tail region of the model. We believe that this increase is a result of lipid exchange between h-POPC in the monolayer and d-DMPC in the nanodiscs.

Figure 3 shows the equivalent data for a DODAB monolayer (15 mN m^{-1}) spread on buffer solutions with and without 100% d-DMPC nanodiscs. The parameters used to generate these SLD profiles are shown in Table 3.

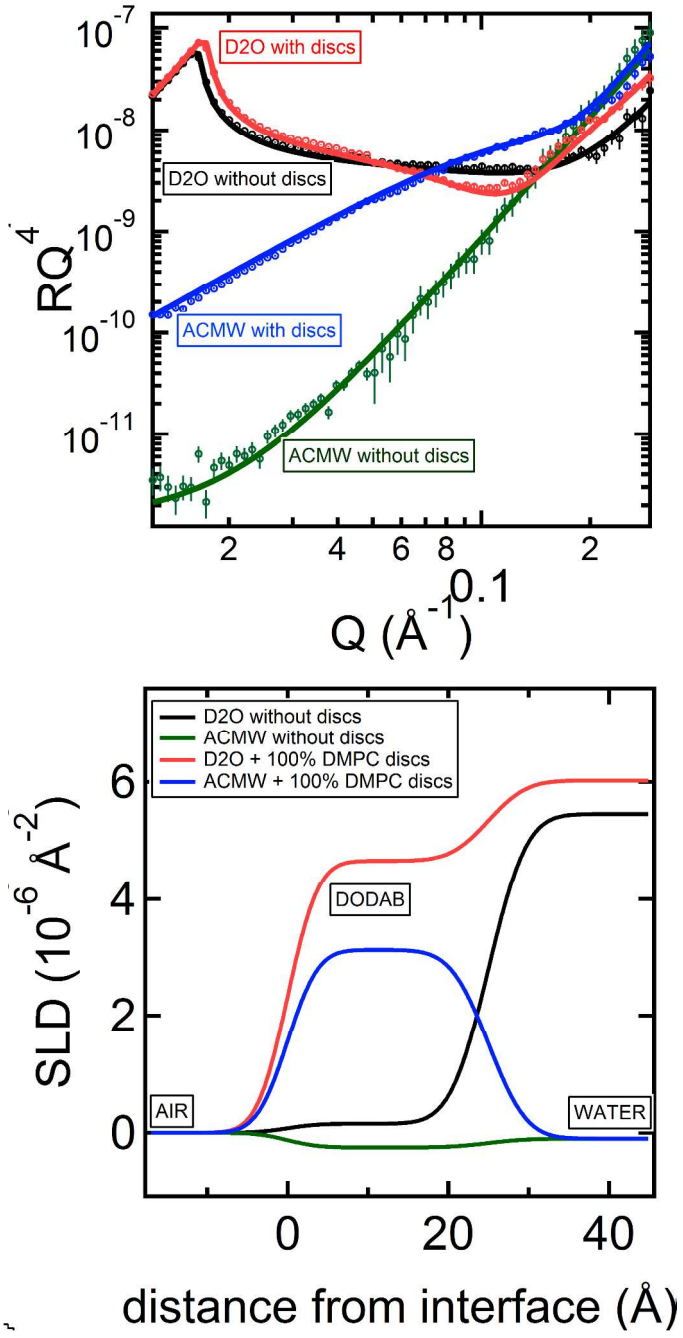

Figure 3- (left) An h-DODAB monolayer on ACMW (dark green) and D_2O (black) buffer contrasts without discs, and on ACMW (blue) and D_2O (red) buffer solution containing 100% d-DMPC nanodiscs. The markers represent the measured reflectometry data and the lines show the calculation from the model SLD profiles shown in (right).

Table 3 Structural parameters obtained from the best fit for h-DODAB monolayers at the surface of buffer solutions with and without nanodiscs (for both D_2O and ACMW contrasts).

Sample	Layer	SLD (x 10^{-6} $Å^{-2}$)	Thickness (Å)	Hydration (%)	Roughness (Å)
Buffer solution without discs	Surface layer (DODAB)	-0.26	25 ± 3	5 ± 5	3 ± 2
	D_2O Sub-phase	5.45	n/a	n/a	4 ± 2
	ACMW Sub-phase	-0.10	n/a	n/a	4 ± 2
Buffer containing 100% d-DMPC disc	Surface layer (DODAB + DMPC)	4.2 ± 0.4	25 ± 2	25 ± 5	3 ± 2
	D_2O Sub-phase	6.02	n/a	n/a	4 ± 2
	ACMW Sub-phase	-0.10	n/a	n/a	4 ± 2

The head group of DODAB is not as large nor strongly scattering as the PC head group and so it is not really appropriate to model this as a separate layer. As such we have been able to fit this layer of DODAB on buffer solution with a single layer. This fit is again consistent with the literature[8], but as for the POPC system, the very weak contrast of the layer means that we cannot be confident in the accuracy of the details of this fit. However, again this weak contrast of the monolayer enhances our sensitivity to the presence at the interface of any deuterated lipid from the nanodiscs.

As with the POPC monolayer, there is a significant difference between the data on buffer solution with and without nanodiscs. In the same way this can only be explained by a large increase in the SLD at the interface. To fit this data we have again considered the addition of a layer to the model that could account for intact nanodisc adsorption. However, applying the same constraints (an unchanged DODAB monolayer and a minimum thickness of ~30 Å for the nanodisc layer), we again cannot find an acceptable fit to the data. In contrast a modelled increase of the SLD of the monolayer can produce an acceptable fit to the data. We again believe that this change is due to the transfer of lipids between the nanodiscs and the monolayer.

Silicon-water

As with the air-water interface we pre-characterized the system prior to injection of nanodiscs. In this case the substrate silicon block coated with OTS was characterized with two water contrasts and then a DOPC lipid monolayer was formed on this surface and further characterized. Figure 4 shows these fits and the details of the parameters used to generate them are summarized in Table 4. The modeled SiO_2 thickness and hydration are comparable to those found in the literature[51]. The thickness of the OTS layer (approximately 27Å), its solvation with water (approximately 12%) and high roughness (9 Å) suggest that it may be incomplete, although the

error on these values are quite high because of the lack of contrast in the measurements used to determine them. The thickness of 27Å is within the range of OTS layers reported in the literature[30] and the roughness is also related to the high roughness of the silicon block used. For the sake of simplicity we have modelled this as a single layer but similar OTS samples have been observed previously and fitted with two layers to give a better agreement across water contrasts[45, 46]. In this case we prefer to minimize the number of fitting parameters and so such detail is approximated by the high roughness of our fit. The DOPC monolayer upon this surface was modelled with an additional layer to account for the head groups, with the hydrogenated-tails incorporated into the same layer as the OTS (although the theoretical SLD of the hydrogenated-tails are slightly different to the OTS layer it is not possible to distinguish these as separate layers, so we have used one value for this layer). The overall thickness of these layers is in reasonable agreement with the literature[52, 53, 54]. The tail thickness can be calculated by comparison with the OTS layer before deposition of the lipid and in our optimum fit is slightly smaller than we might expect, but given the accuracy with which the OTS layer can be determined and the relatively high roughness, this discrepancy can be accounted for and may be due to partial interdigitation of the DOPC tails into the OTS layer. As with the air-water measurements the lack of contrast between protonated lipid tails and the underlying OTS means that we cannot be very confident about the details of this fit. Again though, this contrast does improve the sensitivity to subsequent adsorption of deuterated material.

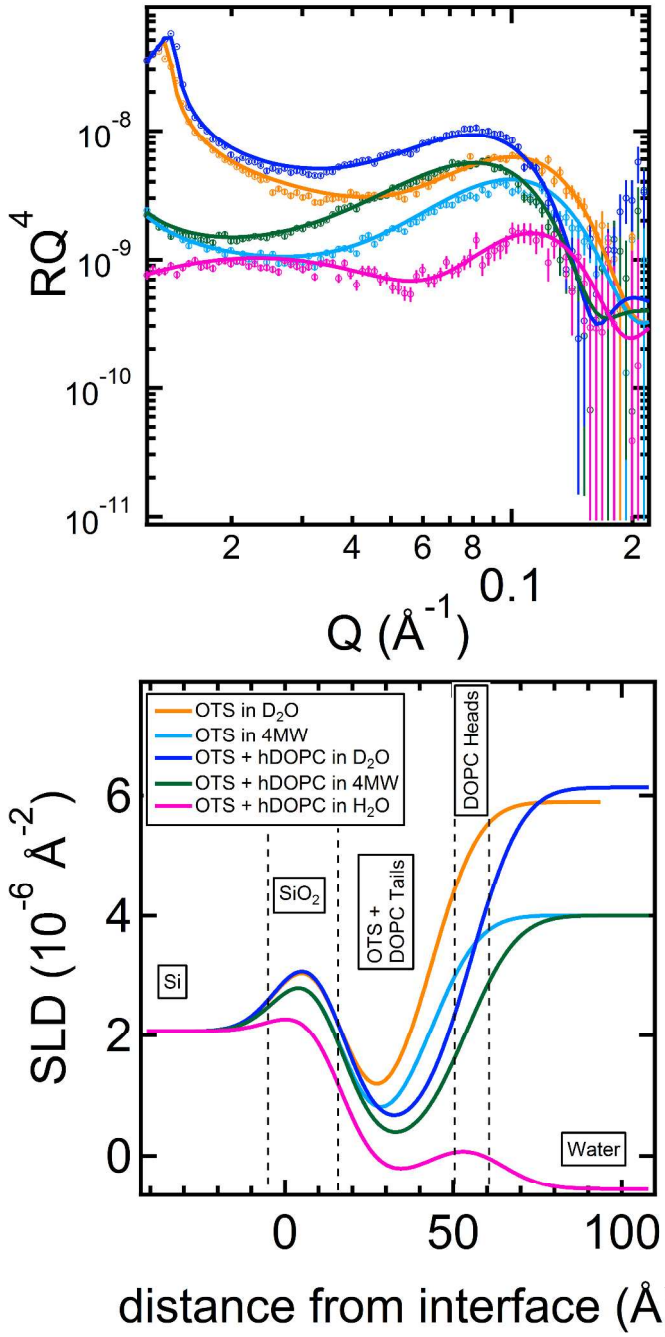

Figure 4- Fits for pre-characterization of OTS and DOPC layers. The data corresponds to bare OTS: orange (in D2O) and light blue (in CM4) and DOPC on OTS: dark blue (in D2O), dark green (in CM4) and pink (in H_2O). The RQ4 scale particularly highlights the variation that is harder to see otherwise.

Table 4: Fit parameters for pre- characterization and after disc injection for d-DMPC discs on to a h-DOPC monolayer at the Silicon-Water interface†

Layer	SLD (x 10^{-6} Å^{-2})	Thickness (Å)	Hydration (%)	Roughness (Å)
Pre-characterization of OTS layer				
Si	2.07			11 ± 3
SiO2	3.47	16± 5	20 ± 10	9 ± 5
OTS	-0.35	27 ± 5	12 ± 5	9 ± 4
h-DOPC monolayer fit prior to disc injection				
OTS + DOPC Tails	-0.35	34± 3	12 ± 5	9 ± 4
DOPC Head	1.80	8 ± 2	10 ± 10	11 ± 3
Monolayer and nanodisc fit after disc injection				
OTS	-0.35	27 ± 5	12 ± 5	8 ± 4
Lipid Tails	3.2 ± 1	7 ± 5	12 ± 12	8 ± 4
Lipid Head group	1.80	8 ± 2	10 ± 10	11 ± 3

The contrasts of water used were H_2O (SLD = -0.56 x 10-6 Å-2), D_2O (SLD = 6.35 x 10-6 Å-2), and "CM4", a mix of H_2O and D_2O (SLD = 4 x 10-6 Å-2). These buffer solutions were pumped through the solid-liquid sample cell, but this did not always achieve full exchange so we have allowed for a minor variation in the SLD of the water.

Figure 5 shows the changes observed in the reflectivity after the addition of 100% d-DMPC nanodiscs for the two water contrasts measured (D_2O and H_2O). As with the air-liquid case, there is a substantial change in the reflectivity. This is most evident for the H_2O contrast where we see a large relative decrease in the reflectivity at Q ≈ 0.05Å and an increase at higher Q. It is also evident in the D_2O contrast, with similar but less dramatic changes to the reflectivity.

Using the same rationale as for the equivalent air-water system, we can conclude that this change is not a result of the simple addition of a fully deuterated nanodisc layer underneath the protonated lipid monolayer. Such a thick layer (≥30Å) consisting of deuterated lipid nanodiscs is not consistent with this observed data. Instead the changes can be almost perfectly modelled by splitting the OTS + lipid tails layer into 2 discrete layers and then simply increasing the SLD of the lipid tails with a small adjustment to the roughness of the two new layers. No other parameters were changed. We conclude that lipid exchange between the nanodiscs and the solid supported monolayer is significant and figure 5 shows our best fit to the observed data using this approach. There are some imperfections in these fits but this is not surprising given the simplicity of the model that we have used. Importantly it is not possible to fit the data using a 3 layer model, while it is possible to marginally improve these fits at high Q by increasing the complexity of the models used. However, we believe that in this case the data does not justify the increased complexity required to improve the fits, since we have limited contrast to fit the hydrogenated lipid monolayer prior to nanodisc adsorption. This was a deliberate strategy in order to increase the sensitivity to adsorbed or exchanged deuteration within the limited beamtime available. Unfortunately it does compromise the precision with which we can determine the exchange, but we feel that any improvements to the fits gained by increasing

model complexity are not appropriate. We therefore prefer to keep the model as simple as possible and qualify our results accordingly.

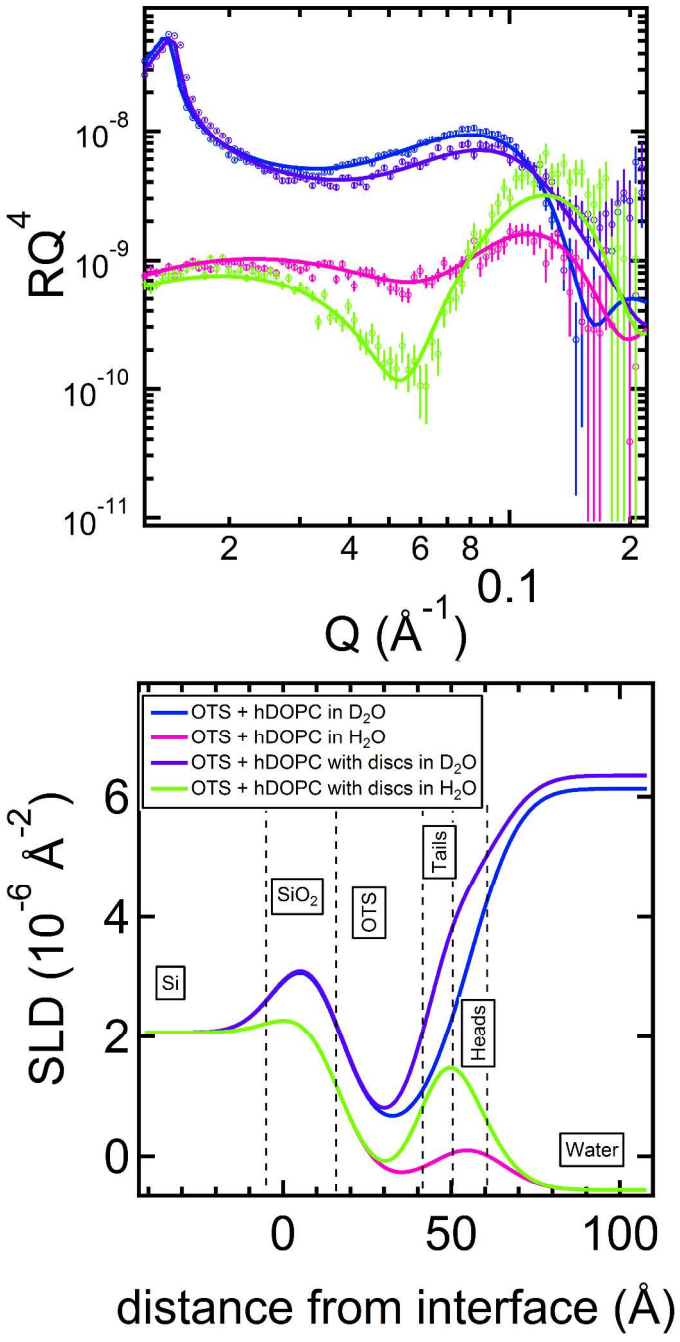

Figure 5- NR data and corresponding fits for solid supported lipid monolayers before (Blue: in D_2O, Pink: in ACMW) and after (Purple in D_2O, Green: in ACMW) lipid exchange with nanodiscs in solution.

Discussion and Conclusions

We have clearly demonstrated that SMALPs will exchange their lipids with a monolayer either at the air-water or silicon-water interface. We believe that there is no other feasible explanation for the changes in reflectivity observed. We cannot determine the mechanism for this exchange from our data, but it is well known that dynamic exchange can occur between micelles[55, 56, 57]. The exchange of lipids between unilamellar DMPC vesicles in solution has also been shown by time-resolved SANS (TR-SANS)[58]. This phenomenon has also recently been shown for protein-stabilized nanodiscs[59]. In these cases it seems that exchange is mediated by monomeric diffusion of lipid through an aqueous medium and not through collisions between nanodiscs. These dynamic properties of lipid exchange between discs are thought to be a consequence of their entropically unstable state, which is a result of lipid confinement through interactions between lipid and polymer/protein. Given the rapid dynamic processes nanodiscs undergo in solution and coupled with the fact that there is an entropic gain when two lipids mix within a monolayer[8], it is reasonable to expect that lipid exchange can explain the observed modification of SLD and the change in surface pressure that we have observed here.

We can use the change in SLD to estimate the volume fraction of lipid exchange between deuterated nanodiscs and hydrogenated monolayers at the air-water interface. The SLD of the interfacial layer can be calculated as:

$$\rho_{monolayer} = (\rho_{hLIPID} \cdot \chi_{hLIPID}) + (\rho_{dLIPID} \cdot \chi_{dLIPID}),$$

where ρ_{hLIPID} and ρ_{dLIPID} are the SLDs of hydrogenated and deuterated lipid within the layer and χ_{hLIPID} and χ_{dLIPID} are their respective volume fractions.

From this equation we can calculate the proportion of lipid exchange in the monolayers at both air-water and solid-liquid interfaces (note that this is only possible for the samples containing 100 % d-DMPC nanodiscs). At the air-water interface it is found that the surface layer is composed of 30 vol % and 60 vol % d-DMPC for lipid exchange between nanodiscs and the h-POPC and h-DODAB monolayers respectively. At the solid-liquid interface it is found that the surface layer is composed of 45 ± 15 vol% d-DMPC after lipid exchange with the h-DOPC monolayer. These very simple models are not perfect since we might expect that the incorporation of d-DMPC into the hydrogenated monolayers would have additional effects on their structure other than the increase in SLD. For example we might also expect the average thickness and roughness of the monolayer to change. Allowing for the variation of these parameters may lead to a better fit to the observed data and marginally alters the best fit for the value of the tail SLD. Such a removal of the constraints between the different water contrasts may also be physically meaningful since it is known that there may be small differences in the behavior of lipids between different water contrasts[60, 61, 62]. However, since we have no other way of constraining such models we have chosen to limit the number of refinable variables used to model this effect. As such the quoted percentage exchange of lipid should be considered an approximate value rather than an absolute quantitative value. We can however, confidently conclude that we see substantial lipid exchange between DMPC nanodiscs and lipid monolayers at the air-water and silicon-water interface. In particular, this exchange is substantially higher than observed in similar experiments using MSP based nanodiscs[61, 62].

The difference in the proportion of lipid exchanged for these systems is probably due to the different electrostatic interactions involved between the lipids. Thus for the lipid exchange into the cationic DODAB monolayer, repulsion between the lipids is reduced by the incorporation of zwitterionic DMPC. For the nanodiscs containing 20 mol % DMPG, however, we believe that there is an entropic stabilization in the fact that the nanodiscs already contain mixed lipids, which reduces the driving force for lipid exchange[8].

As far as we can tell any nanodisc adsorption is weak under these conditions of time, temperature, pH and ionic strength. It seems likely that any adsorption of nanodiscs to the monolayers is likely to be in dynamic equilibrium since coverage is not high enough to be resolved in our data and because the lipid exchange is very high in some cases. This does not mean that adsorption is not possible for these systems, but does suggest that the process is more sensitive to conditions than for MSP based nanodiscs.

Ultimately an understanding of this behavior will be important for many applications of SMALP technology. The current assumption that a protein is extracted from a native membrane is not necessarily maintained during a multiple step purification process. Similarly it is potentially possible to control the lipid environment surrounding SMALPed proteins, and thereby gain an understanding of the role that these lipids play in membrane protein function. To achieve this aim it is essential to gain a more detailed understanding of the factors that govern lipid exchange. We are now investigating further the extent of this behavior by directly examining the kinetics of lipid exchange from nanodiscs (with and without incorporated proteins) as a function of the polymer, lipid and solution conditions using a range of different techniques.

Supporting Information. The electronic supplementary information for this article includes GPC and NMR for confirmation of polymer synthesis and DLS for confirmation of the nanodisc formation. This material is available free of charge via the Internet at http://pubs.acs.org.

AUTHOR INFORMATION

Corresponding Author

* tom.arnold@diamond.ac.uk

Present Addresses

†School of Oral and Dental Sciences, University of Bristol, Lower maudlin Street, Bristol, BS1 2LY, U.K.

ACKNOWLEDGMENT

The authors would like to thank Stephen Hall, Tim Dafforn and Dr Max Skoda for their assistance with some related work and ISIS for beamtime (RB1410558 and RB1320372). GH would like to thank the University of Bath and Diamond Light Source for funding.

REFERENCES

1. Orwick, M. C.; Judge, P. J.; Procek, J.; Lindholm, L.; Graziade, A.; Engel, A.; Grobner, G.; Watts, A. Detergent-free formation and physiochemical characterisation of nanosized lipid-polymer complexes: Lipodisq. *Angewandte Chemie* **2012,** *124* (19), 4731-4735.

2. Nath, A.; Atkins, W. M.; Sligar, S. G. Applications of phospholipid bilayer nanodiscs in the study of membranes and membrane proteins. *Biochemistry* **2007,** *46* (9), 2060-2069.

3. Inagaki, S.; Ghirlando, R.; Grisshammer, R. Biophysical characterization of membrane proteins in nanodiscs. *Methods in enzymology* **2013,** *59* (3), 287-300.

4. Arinaminpathy, Y.; Khurana, E.; Engelman, D. M.; Gerstein, M. B. Computational analysis of membrane proteins: the largest class of drug targets. *Drug discovery today* **2009,** *23* (24), 1130-1135.

5. Carpenter, E. P.; Beis, K.; Cameron, A. D.; Iwata, S. Overcoming the challenges of membrane protein crystallography. *Current opinion in structural biology* **2008,** *18* (5), 581-586.

6. Wadsäter, M.; Barker, R.; Mortensen, K.; Feidenhans'l, R.; Cárdenas, M. Effect of Phospholipid Composition and Phase on Nanodisc Films at the Solid–Liquid Interface as Studied by Neutron Reflectivity. *Langmuir* **2013,** *29* (9), 2871-2880.

7. Wadsater, M.; Lauridsen, T.; Singha, A.; Hatzakis, N. S.; Stamou, D.; Barker, R.; Mortensen, K.; Feidenhaus'l, R.; Moller, B. L.; Cardenas, M. Monitoring shifts in the conformation equilibrium of the membrane protein cytochrome P450 reductase (POR) in nanodiscs. *The journal of biological chemistry* **2012,** *287*, 34596-34603.

8. Wadsäter, M.; Simonsen, J. B.; Lauridsen, T.; Tveten, E. G.; Naur, P.; Bjørnholm, T.; Wacklin, H.; Mortensen, K.; Arleth, L.; Feidenhans'l, R.; Cárdenas, M. Aligning Nanodiscs at the Air–Water Interface, a Neutron Reflectivity Study. *Langmuir* **2011,** *27* (24), 15065-15073.

9. Bayburt, T. H.; Carlson, J. W.; Sligar, S. G. Reconstitution and imaging of a membrane protein in a nanometer-size phospholipid bilayer. *J Struct Biol* **1998,** *123* (1), 37-44.

10. Carlson, J. W.; Jones, A. L.; Sligar, S. G. Imaging and manipulation of high-density lipoproteins. *Biophysical Journal* **1997,** *73* (3), 1184-1189.

11. Lipfert, J.; Doniach, S. Small-angle x-ray scattering from RNA, proteins and protein complexes. *Annual Review of Biophysics and Biomolecular Structure* **2007,** *36*, 307-327.

12. Bayburt, T. H.; Sligar, S. G. Membrane protein assembly into Nanodioscs. *FEBS Letters* **2010,** *584* (9), 1721-1727.

13. Denisov, I. G.; Grinkova, Y. V.; Lazarides, A. A.; Sligar, S. G. Directed self-assembly of monodisperse phospholipid bilayer nanodiscs with controlled size. *Journal of the American Chemical Society* **2004,** *126* (11), 3477-3487.

14. Gislinge, S.; Arleth, L. Small-angle scattering from phospholipid nanodiscs: derivation and refinement of a molecular constrained analytical model form factor. *Physical Chemistry Chemical Physics* **2011,** *28* (13), 3161-3170.

15. Dutta, P. Grazing Incidence X-ray Diffraction. *Current Science* **2000,** *78* (12), 1478-1484.

16. Zhou, X. L.; Chen, S. W. Theoretical foundation of x-ray and neutron reflectometry. *Physics Reports* **1995,** *257* (4-5), 223-348.

17. Bertram, N.; Laursen, T.; Barker, R.; Bavishi, K.; Lindberg, B. L.; Cardenas, M. Nanodisc films for membrane protein studies by neutron reflection: Effect of the protein scaffold choice. *Langmuir* **2015,** *31*, 8386-8391.

18. Jamshad, M.; Grimard, V.; Idini, I.; Knowles, T.; Dowle, M.; Schofield, N.; Sridhar, P.; Lin, Y.; Finka, R.; Wheatley, M.; Thomas, O. T.; Palmer, R.; Overduin, M.; Govaerts, C.; Ruysschaert, J.-M.; Edler, K.; Dafforn, T. Structural analysis of a nanoparticle containing a lipid bilayer used for detergent-free extraction of membrane proteins. *Nano Res.* **2014**, 1-16.

19. Jamshad, M.; Lin, Y. P.; Knowles, T. J.; Parslow, R. A.; Harris, C.; Wheatley, M.; Poyner, D. R.; Bill, R. M.; Thomas, O. R.; Overduin, M.; Dafforn, T. R. Surfactant-free purification of membrane proteins with intact native membrane environment. *Biochem Soc Trans* **2011,** *39* (3), 813-8.

20. Knowles, T. J.; Finka, R.; Smith, C.; Lin, Y. P.; Daffron, T.; Overduin, M. Membrane Proteins Solubilized Intact in Lipid Containing Nanoparticles Bounded by Styrene Maleic Acid Copolymer. *Journal of the American Chemical Society* **2012,** *131* (22).

21. Paulin, S.; Jamshad, M.; Dafforn, T. R.; Garcia-Lara, J.; Foster, S. J.; Galley, N. F.; Roper, D. I.; Rosado, H.; Taylor, P. W. Surfactant-free purification of membrane protein complexes from bacteria: application to the staphylococcal penicillin-binding protein complex PBP2/PBP2a. *Nanotechnology* **2014,** *25* (28), 5101.

22. Lee, S. C.; Knowles, T. J.; Postis, V. L. G.; Jamshad, M.; Parslow, R. A.; Lin, Y.-p.; Goldman, A.; Sridhar, P.; Overduin, M.; Muench, S. P.; Dafforn, T. R. A method for detergent-free isolation of membrane proteins in their local lipid environment. *Nat. Protocols* **2016,** *11* (7), 1149-1162.

23. Phillips, R.; Ursell, T.; Wigging, P.; Sens, P. Emerging role of lipids in shaping membrane-protein funcion. *Nature* **2009,** *459*, 379-385.

24. Andersen, O. S.; Koeppe, R. E. Bilayer thickness and membrane protein function: An energetic perspective. *Biophysics* **2007,** *36*, 107-130.

25. Harrison, S.; Wooley, K. L. Shell-crosslinked nanostructures from amphiphilic AB and ABA block co-polymers of styrene-alt-(maleic anhydride) and styrene: polymerisation, assembly and stabilisation in one pot. *Chemical Communications* **2005,** *26*, 3259-3261.

26. Daillant, J.; Gibaud, A. *X-ray and Neutron Reflectivity*; Springer-Verlag Berlin Heidelberg2009.

27. **D.S., S.** *Elementary Scattering Theory for X-ray and Neutron Users*; OUP2011.

28. Majkrzak, C. F.; Satija, S.; Berk, N. F.; Krueger, S.; Borchers, J. A.; Dura, J. A.; Ivkov, R.; O'donovan, K. V. Neutron reflectometry at the NCNR. *Neutron News* **2001,** *12* (2), 25-29.

29. Jamshad, M.; Grimard, V.; Idini, I.; Knowles, T. J.; Dowle, M. R.; Schofield, N.; Sridhar, P.; Lin, Y.-P.; Finka, R.; Wheatley, M.; Thomas, O. T.; Palmer, R. E.; Overduin, M.; Govaerts, C.; Ruysschaert, J.; Edler, K. J.; Dafforn, T. R. Structural analysis of a nanoparticle containing a lipid bilayer used for detergent free extraction of membrane proteins. *Nano Research* **2014,** *8*, 774-789.

30. Hollinsead, C. M.; Hanna, M.; Barlow, D. J.; Biasi, V. D.; Bucknall, D. G.; Camilleri, P.; Hutt, A. J.; Lawrence, M. J.; Lu, J. R.; Sun, J. T. Neutron reflection from a dimyristoylphosphatidylcholine monolayer adsorbed on a hydrophobised silicon support. *Biochimica et Biophysica Acta* **2001,** *1511*, 49-59.

31. Akesson, A.; Lind, T.; Ehrlich, N.; Stamou, D.; Wacklin, H. P.; Cardenas, M. Composition and structure of mixed phospholipid supported bilayers formed by POPC and DPPC. *Soft Matter* **2012,** *8*, 5658-5665.

32. Wacklin, H. P.; Tiberg, F.; Fragneto, G.; Thomas, R. L. Phospholipase A2 hydrolysis of supported phospholipid bilayers: A neutron reflectivity and ellipsometry study. *Biochemistry* **2005,** *44*, 2811-2821.

33. Dabkowska, A.; Barlow, D. J.; Campbell, R. A.; Hughes, A. V.; Quinn, P. J.; Lawrence, M. J. Effect of helper lipids on the interaction of DNA with cationic lipid monolayers studied by specular neutron reflection. *Biomacromolecules* **2012,** *13* (8), 2391-2401.

34. Kucerka, N.; Kiselev, M. A.; Balgavy, P. Determination of bilayer thickness and lipid surface area in unilamellar dimyristoylphosphatidylcholine vesicles from small-angle neutron scattering curves: a comparison of evaluation methods. *European Biophysics Journal with Biophysics Letters* **2004,** *33* (4), 328-334.

35. Marsh, D. Molecular volumes of lipids and glycolipids in membranes. *Chemistry and Physics of Lipids* **2010,** *163* (7), 667-677.

36. Fragneto, G.; Thomas, R. K.; Rennie, A. R.; Penfold, J. Neutron reflection study of bovine B-casein adsorbed on OTS self-assembled monolayers. *Science* **1995,** *267*, 657-660.

37. Fenzl, W.; Sigl, L.; Richardsen, H.; Cevc, G. The surface-confined structures of dimyristoylphosphatidylcholine bilayers in contact with the vesicle suspension as studied by means of X-ray reflectivity. *Colloids and Surfaces A: Physicochemical and Engineering Aspects* **1995,** *102* (0), 247-256.

38. Kahn, J. G.; Monroy, F.; Mingotaud, C. Adsorption of large inorganic polyanions under a charged Langmuir monolayer: an ellipsometric study. *Physical Chemistry Chemical Physics* **2003,** *5* (2648-2652).

39. Webster, J.; Holt, S.; Dalgliesh. INTER the chemical interfaces reflectometer on target station 2 at ISIS. *Physica B* **2006,** *385*, 1164-1166.

40. Dalgliesh, R. M.; Langridge, S.; Plomp, J.; de Haan, V. O.; van Well, A. A. Offspec, the ISIS spin-echo reflectometer. *Physica B: Condensed Matter* **2011,** *406* (12), 2346-2349.

41. Nelson, A. Co-refinement of multiple-contrast neutron/x-ray reflectivity data using MOTOFIT. *Journal of Applied Crystallography* **2006,** *39* (2), 273-276.

42. Born, M.; Wolf, E. *Principles of Optics*; Pergamon: Oxford, 1970.

43. Abeles, F. Investigations on the propagation of sinusoidal electromagnetic waves in stratified media: application to thin films. *Annals of physics* **1948,** *3*, 504-520.

44. Karst, J. C.; Barker, R.; Devi, U.; Swann, M. J.; Davi, M.; Roser, S. J.; Ladant, D.; Chenal, A. Identification of a region that assists membrane insertion and translocation of the catalytic domain of bordetella pertussis CyA toxin. *Journal of Biological Chemistry* **2012,** *287*, 9200-9212.

45. Fragneto, G.; Li, Z. X.; Thomas, R. K.; Rennie, A. R.; Penfold, J. A Neutron Reflectivity Study of the Adsorption of Aerosol-OT on Self-Assembled Monolayers on Silicon. *Journal of Colloid and Interface Science* **1996,** *178* (2), 531-537.

46. Fragneto, G.; Thomas, R.; Rennie, A.; Penfold, J. Neutron reflection study of bovine beta-casein adsorbed on OTS self-assembled monolayers. *Science* **1995,** *267* (5198), 657-660.

47. Lingler, S.; Rubinstein, I.; Knoll, W.; Offenhausser. Fusion of small unilamellar lipid vesicles to alkanethiol and thiolipid self-assembled monolayers on gold. *Langmuir* **1997,** *13* (26), 7085-7091.

48. Keller, C. A.; Kasemo, B. Surface specific kinetics of lipid vesicle adsorption measured with a quartz crystal microbalance. *Biophysical Journal* **1998,** *75*, 1397-1402.

49. Idini, I. PhD. PhD, University of Bath, July 2014 2014.

50. Wacklin, H. P.; Tiberg, F.; Thomas, R. K. Formation of supported phospholipid bilayers via co-adsorption with B-D-dodecyl maltoside. *Biochimica et Biophysica Acta* **2005,** *1668*, 17-24.

51. Dura, J. A.; Richter, C. A.; Majkrzak, C. F.; Nguyen, N. V. Neutron reflectometry, x-ray reflectometry, and spectroscopic ellipsometry characterization of thin SiO2 on Si. *Applied Physics Letters* **1998,** *73* (15), 2131-2133.

52. Vacklin, H. P.; Tiberg, F.; Thomas, R. K. Formation of supported phospholipid bilayers via co-adsorption with β-d-dodecyl maltoside. *Biochimica et Biophysica Acta (BBA) - Biomembranes* **2005,** *1668* (1), 17-24.

53. Vaknin, D.; Kjaer, K.; Als-Nielsen, J.; Lösche, M. Structural properties of phosphatidylcholine in a monolayer at the air/water interface. *Biophysical Journal* **1991,** *59* (6), 1325-1332.

54. Miller, C. E.; Majewski, J.; Gog, T.; Kuhl, T. L. Characterization of Biological Thin Films at the Solid-Liquid Interface by X-Ray Reflectivity. *Physical Review Letters* **2005,** *94* (23), 238104.

55. Lund, R.; Willner, L.; Richter, D.; Dormidontova, E. E. Equilibrium chain exchange kinetics of diblock co-polymer micelles: Tuning and logarithmic relaxation. *Macromolecules* **2006,** *39* (13), 4566-4575.

56. Lund, R.; Willner, L.; Stellbrink, J.; Lindner, P.; Richter, D. Logarithmic chain-exchange kinetics of diblock copolymer micelles. *Physical Review Letters* **2006,** *96* (104), 068302.

57. Willner, L.; Poppe, A.; Allgaier, J.; Monkenbusch, M.; Richter, D. Time-resolved SANS for the determination of unimer exchange kinetics in block co-polymer micelles. *Europhysics Letters* **2001,** *55* (5), 667-673.

58. Nakano, M.; Fukuda, M.; Kudo, T.; Endo, H.; Handa, T. Determination of interbilayer and transbilayer lipid transfers by time-resolved small-angle neutron scattering. *Phys Rev Lett* **2007,** *98* (23), 238101.

59. Nakano, M.; Fukuda, M.; Kudo, T.; Miyazaki, M.; Wada, Y.; Matsuzaki, N.; Endo, H.; Handa, T. Static and Dynamic Properties of Phospholipid Bilayer Nanodiscs. *Journal of the American Chemical Society* **2009,** *131* (23), 8308-8312.

60. Fragneto, G.; Thomas, R. K. Neutron reflection from hexadecyltrimethylammonium bromide adsorbed on smooth and rough silicon surfaces. *Langmuir* **1996,** *12* (25), 6036-6043.

61. Wadsater, M.; Barker, R.; Mortensen, K.; Feidenhaus'l, R.; Cardenas, M. Effect of phospholipid composition and phase on nanodisc films at the solid-liquid interface as studied by neutron reflectivity. *Langmuir* **2013,** *13* (29), 2871-2880.

62. Wadsater, M.; Simonsen, J. B.; Lauridsen, T.; Tveten, E. G.; Naur, P.; Bjornholm, T.; Wacklin, H.; Mortensen, K.; Arleth, L.; Feidenhaus'l, R.; Cardenas, M. Aligning nanodiscs at the air-water interface, a neutron reflectivity study. *Langmuir* **2011,** *27* (24), 15065-15073.

TOC Image